[6]Ardema, M. D., "Singular Perturbations in Flight Mechanics," NASA TM X-62380, 1974.
[7]Lu, P., "Analytical Solution to Constrained Hypersonic Trajectories," *Journal of Guidance, Control, and Dynamics*, Vol. 16, No. 5 1993, pp. 956–960.
[8]Warren, A., "Application of Total Energy Control for High-Performance Aircraft Vertical Transition," *Journal of Guidance, Control, and Dynamics*, Vol. 14, No. 2 1991, pp. 447–452.
[9]Bugajski, D. J., and Enns, D. F., "Nonlinear Control Law with Application to High Angle-of-Attack Flight," *Journal of Guidance, Control, and Dynamics*, Vol. 15, No. 3, 1992, pp. 761–767.
[10]Snell, S. A., Enns, D. F., and Garrard, W. F., "Nonlinear Inversion Flight Control for a Supermaneuverable Aircraft," *Journal of Guidance, Control, and Dynamics*, Vol. 15, No. 4, 1992, pp. 976–984.
[11]Shtessel, Y., Hall, C., and Jackson, M., "Reusable Launch Vehicle Control in Multiple Time Scale Sliding Modes," *Journal of Guidance, Control, and Dynamics*, Vol. 23, No. 6, 2000, pp. 1013–1020.
[12]Lu, P., "Constrained Tracking Control of Nonlinear Systems," *Systems and Control Letters*, Vol. 27, 1996, pp. 305–314.
[13]Lu, P., "Approximate Nonlinear Receding-Horizon Control Laws in Closed Form," *International Journal of Control*, Vol. 71, No. 1, 1998, pp. 19–34.
[14]O'Malley, R. E., Jr., "On Nonlinear Singularly Perturbed Initial Value Problems," *SIAM Review*, Vol. 30, No. 2, 1988, pp. 193–212.
[15]Khalil, H. K., *Nonlinear Systems*, 2nd ed., Prentice–Hall, Upper Saddle River, NJ, 1996, pp. 351–388.
[16]Harpold, J. C., and Graves, C. A., "Shuttle Entry Guidance," *The Journal of the Astronautical Sciences*, Vol. 37, No. 3, 1979, pp. 239–268.
[17]Bharadwaj, S., Rao, A. V., and Mease, K. D., "Entry Trajectory Tracking Law via Feedback Linearization," *Journal of Guidance, Control, and Dynamics*, Vol. 21, No. 5, 1998, pp. 726–732.
[18]Lu, P.,"Regulation About Time-Varying Trajectories: Precision Entry Guidance Illustrated," *Journal of Guidance, Control, and Dynamics*, Vol. 22, No. 6, 1999, pp. 784–790.

# Nonlinear Tracking Control of an Underactuated Spacecraft

A. Behal* and D. Dawson†
*Clemson University, Clemson, South Carolina 29634-0915*
E. Zergeroglu‡
*OFS Fitel, Sturbridge, Massachusetts 01566*
and
Y. Fang§
*Clemson University, Clemson, South Carolina 29634-0915*

## Introduction

RECENTLY, there has been some interest in designing controllers for the underactuated rigid spacecraft tracking/stabilization problem. In Ref. 1, Crouch provided necessary and sufficient conditions for controllability of a rigid body in the case of one, two, or three independent actuators. In Ref. 2, Byrnes and Isidori demonstrated that a rigid spacecraft with only two controls cannot be asymptotically stabilized via continuous-state feedback because it does not satisfy Brockett's necessary condition[3] for smooth feedback stabilizability. In Ref. 4, Morin et al. developed a smooth, time-varying stabilizing controller by using averaging theory. A continuous time-varying/time-periodic switching controller was proposed by Coron and Kerai in Ref. 5. When averaging theory and Lyapunov control design techniques were used, Morin and Samson[6] developed a continuous time-varying controller that locally exponentially stabilized the attitude of a rigid spacecraft. Recently, in Ref. 7, Tsiotras and Luo proposed a saturated, tracking/stabilizing controller for the kinematic control of an underactuated axisymmetric spacecraft; however, the spin rate on the unactuated axis is required to be zero.

In this Note, we propose a novel, continuous, time-varying, nonlinear tracking controller for the kinematic model of an axisymmetric as well as nonaxisymmetric underactuated rigid spacecraft. The control structure is motivated by the Lyapunov-based dynamic oscillator presented in Ref. 8 for wheeled mobile robots. The proposed control approach is novel in that several key characteristics of the quaternion kinematic representation are exploited during the redesign of the control structure originally proposed in Ref. 8. Indeed, it is the fusion of the dynamic oscillator-based approach, that is, it provides additional design flexibility, and quaternion kinematic representation that facilitates the tracking result for the underactuated spacecraft system. The controller ensures that the spacecraft orientation error is driven to an arbitrarily small neighborhood of zero provided the initial errors are sufficiently small, that is, the controller guarantees local uniform, ultimately bounded (LUUB) tracking with exponential convergence. Standard backstepping control techniques can be fused with the kinematic controller to present a solution, that is, both dynamic and kinematic effects can be accounted for, for full-order LUUB tracking/regulation of an axisymmetric spacecraft. In contrast to the work presented in Ref. 7, the axisymmetric control strategy is for the full-order model; furthermore, it does not impose restrictions on the spin rate of the unactuated axis.

## Problem Formulation

The kinematics for a rigid spacecraft can be expressed as follows[9]:

$$\dot{\boldsymbol{q}} = \tfrac{1}{2}(q^{\times}\omega + q_0\boldsymbol{\omega}) \tag{1}$$

$$\dot{q}_0 = -\tfrac{1}{2}\boldsymbol{q}^T\boldsymbol{\omega} \tag{2}$$

where $\boldsymbol{\omega}(t) \in \Re^3$ is the angular velocity of a body-fixed reference frame $\mathcal{F}$ (located at the center of mass of the spacecraft) with respect to an inertial reference frame $\mathcal{I}$, the notation $\zeta^{\times}$, $\forall\zeta = [\zeta_1 \;\; \zeta_2 \;\; \zeta_3]^T$, denotes the following skew-symmetric matrix:

$$\zeta^{\times} = \begin{bmatrix} 0 & -\zeta_3 & \zeta_2 \\ \zeta_3 & 0 & -\zeta_1 \\ -\zeta_2 & \zeta_1 & 0 \end{bmatrix} \tag{3}$$

and $\boldsymbol{q}_E(t) \triangleq \{q_0(t), \boldsymbol{q}(t)\} \in \Re \times \Re^3$ represents the unit quaternion[9] describing the orientation of the body-fixed frame $\mathcal{F}$ with respect to the inertial frame $\mathcal{I}$, which is subject to the constraint $\boldsymbol{q}^T\boldsymbol{q} + q_0^2 = 1$. The rotation matrix that brings $\mathcal{I}$ onto $\mathcal{F}$, denoted by $R(\boldsymbol{q}, q_0) \in \Re^{3\times 3}$, is defined as

$$R \triangleq \left(q_0^2 - \boldsymbol{q}^T\boldsymbol{q}\right)I_3 + 2\boldsymbol{q}\boldsymbol{q}^T - 2q_0\boldsymbol{q}^{\times} \tag{4}$$

where $I_3$ is the $3 \times 3$ identity matrix and the angular velocity of $\mathcal{F}$ with respect to $\mathcal{I}$ expressed in $\mathcal{F}$ is $\boldsymbol{\omega}(t)$.

We assume that the desired attitude of the spacecraft can be described by a desired, body-fixed reference frame $\mathcal{F}_d$ whose orientation with respect to the inertial frame $\mathcal{I}$ is specified by the desired unit quaternion $\boldsymbol{q}_{dE}(t) = \{q_{0d}(t), \boldsymbol{q}_d(t)\} \in \Re \times \Re^3$ that is constructed to satisfy $\boldsymbol{q}_d^T\boldsymbol{q}_d + q_{0d}^2 = 1$. The corresponding rotation matrix, denoted by $R_d(\boldsymbol{q}_d, q_{0d}) \in \Re^{3\times 3}$, that brings $\mathcal{I}$ onto $\mathcal{F}_d$ is then defined as

$$R_d = \left(q_{0d}^2 - \boldsymbol{q}_d^T\boldsymbol{q}_d\right)I_3 + 2\boldsymbol{q}_d\boldsymbol{q}_d^T - 2q_{0d}\boldsymbol{q}_d^{\times} \tag{5}$$

Received 12 June 2001; revision received 18 October 2001; accepted for publication 20 May 2002. 

*Postdoctoral Fellow, Department of Bioengineering; abehal@ces.clemson.edu.
†Professor, Department of Electrical and Computer Engineering; ddawson@ces.clemson.edu.
‡Controls Engineer, Department of Controls and Software Engineering; ezerger@ofsoptics.com.
§Graduate Student, Department of Electrical and Computer Engineering; yfang@clemson.edu.

The desired quaternion is related to the desired angular velocity of $\mathcal{F}_d$ with respect to $\mathcal{I}$ expressed in $\mathcal{F}_d$, denoted by $\bar{\omega}_d(t) \in \Re^3$, through the following dynamic equations:

$$\dot{\boldsymbol{q}}_d = \tfrac{1}{2}\left(q_d^\times \bar{\boldsymbol{\omega}}_d + q_{0d}\bar{\boldsymbol{\omega}}_d\right) \tag{6}$$

$$\dot{q}_{0d} = -\tfrac{1}{2}\boldsymbol{q}_d^T \bar{\boldsymbol{\omega}}_d \tag{7}$$

where Eqs. (6) and (7) can be inverted to calculate $\bar{\omega}_d(t)$ as

$$\bar{\boldsymbol{\omega}}_d = 2(q_{0d}\dot{\boldsymbol{q}}_d - \boldsymbol{q}_d\dot{q}_{0d}) - 2q_d^\times \dot{\boldsymbol{q}}_d \tag{8}$$

To quantify the mismatch between the actual and desired spacecraft attitudes, we define the rotation matrix $\tilde{R}(e, e_0) \in \Re^{3\times 3}$ that brings $\mathcal{F}_d$ onto $\mathcal{F}$ as

$$\tilde{R} = RR_d^T = \left(e_0^2 - \boldsymbol{e}^T\boldsymbol{e}\right)I_3 + 2\boldsymbol{e}\boldsymbol{e}^T - 2e_0e^\times \tag{9}$$

where the quaternion tracking error $\boldsymbol{e}_E(\boldsymbol{t}) \triangleq \{e_0(t), \boldsymbol{e}(\boldsymbol{t})\} \in \Re \times \Re^3$ is defined as

$$e_0 = q_0q_{0d} + \boldsymbol{q}^T\boldsymbol{q}_d \tag{10}$$

$$\boldsymbol{e} = q_{0d}\boldsymbol{q} - q_0\boldsymbol{q}_d + q^\times \boldsymbol{q}_d \tag{11}$$

Based on the preceding tracking error formulation, we define the angular velocity of $\mathcal{F}$ with respect to $\mathcal{F}_d$ expressed in $\mathcal{F}$, denoted by $\tilde{\boldsymbol{\omega}}(t) = [\tilde{\omega}_1(t) \quad \tilde{\omega}_2(t) \quad \tilde{\omega}_3(t)] \in \Re^3$, as

$$\tilde{\boldsymbol{\omega}} = \boldsymbol{\omega} - \boldsymbol{\omega}_d \tag{12}$$

where $\boldsymbol{\omega}_d(\boldsymbol{e}, e_0, t) = [\omega_{d1}(\cdot) \ \ \omega_{d2}(\cdot) \ \ \omega_{d3}(\cdot)] \in \Re^3$ is an auxiliary variable that is defined as

$$\boldsymbol{\omega}_d = \tilde{R}\bar{\boldsymbol{\omega}}_d \tag{13}$$

where $\tilde{R}(\boldsymbol{e}, e_0)$ and $\bar{\boldsymbol{\omega}}_d(t)$ were defined in Eqs. (9) and (8), respectively. We can now compute the open-loop tracking error dynamics as

$$\dot{\boldsymbol{e}} = \tfrac{1}{2}(e^\times + e_0I_3)\tilde{\boldsymbol{\omega}} \tag{14}$$

$$\dot{e}_0 = -\tfrac{1}{2}\boldsymbol{e}^T\tilde{\boldsymbol{\omega}} \tag{15}$$

*Remark 1:* After the utilization of the actual and desired unit quaternion constraints as well as Eqs. (10) and (11), it is seen that the quaternion tracking error variables satisfy the following constraint:

$$\boldsymbol{e}^T\boldsymbol{e} + e_0^2 = 1 \tag{16}$$

*Remark 2:* The open-loop kinematic tracking error system has been formulated as though the desired trajectory input, denoted by $\boldsymbol{q}_d(t)$, is provided by a trajectory planning module. [Note that $q_{0d}(t)$ can be calculated via $q_{0d}^2 = 1 - \boldsymbol{q}_d^T\boldsymbol{q}_d$.] However, we note that the trajectory planning module can also provide $\bar{\omega}_d(t)$ as the desired trajectory input with $\boldsymbol{q}_d(t)$ and $q_{0d}(t)$ being calculated by a reference trajectory generator in the form of Eqs. (6) and (7).

*Remark 3:* Based on the definition given by Eq. (9), the attitude control objective is achieved if $\tilde{R}(t) = I_3$. It is easy to see from Eq. (16) that, if $\boldsymbol{e}(\boldsymbol{t}) = 0$, then $|e_0(t)| = 1$; hence, we can see from Eq. (9) that if $\boldsymbol{e}(\boldsymbol{t}) = 0$, then $\tilde{R}(t) = I_3$. Based on this argument, it is easy to see that the attitude control objective is to drive $\boldsymbol{e}(t)$ to zero (or to some small value). With regard to achieving this control objective, we make the standard assumption that $q_{0d}(t)$, $\boldsymbol{q}_d(t)$, and their first two time derivatives are bounded for all time.

Because we are interested in designing a controller for the attitude control problem, we will first develop a kinematic tracking controller. Specifically, we will assume that $\omega_2(t)$ and $\omega_3(t)$ are the control inputs. We also assume that $\boldsymbol{q}_E(t)$ is measurable and that $\omega_1(t)$ is a measurable, exogenous, bounded signal. To facilitate the underactuated control design process, we rewrite Eqs. (14) and (15) in a manner conducive to the stability analysis as follows:

$$\dot{\boldsymbol{x}} = \tfrac{1}{2}\left(f + z^TJ_2\boldsymbol{u}\right) \tag{17}$$

$$\dot{z} = \tfrac{1}{2}\left(J_2z\tilde{\omega}_1 - B[\omega_{d2} \quad \omega_{d3}]^T + B\boldsymbol{u}\right) \tag{18}$$

where $x(t) \in \Re^1$, $z(t) = [e_2(t) \ \ e_3(t)]^T \in \Re^2$ are the transformed error signals that are related to the original open-loop tracking error variable $\boldsymbol{e}(t) \in \Re^3$ of Eq. (11) as follows:

$$x = e_1 \qquad z = [e_2 \quad e_3]^T \tag{19}$$

The auxiliary signal $f(t) \in \Re^1$ is defined as

$$f = e_0\tilde{\omega}_1 - e_2\omega_{d3} + e_3\omega_{d2} \tag{20}$$

where $\omega_{d2}(\cdot)$, $\omega_{d3}(\cdot)$ were introduced in Eq. (13), $B(e_0, e_1) \in \Re^{2\times 2}$ is a matrix that is defined as

$$B = \begin{bmatrix} e_0 & -e_1 \\ e_1 & e_0 \end{bmatrix} \tag{21}$$

$J_2 \in \Re^{2\times 2}$ is a skew-symmetric matrix that is defined as

$$J_2 = \begin{bmatrix} 0 & 1 \\ -1 & 0 \end{bmatrix} \tag{22}$$

and $\boldsymbol{u}(t) = [\omega_2(t) \ \ \omega_3(t)] \in \Re^2$ is the kinematic control input vector.

## Kinematic Control Design

Our control objective is the design of a kinematic controller that exponentially drives the tracking error system of Eqs. (17) and (18) to a neighborhood about zero that can be made arbitrarily small. To this end, we define an auxiliary error signal $\tilde{z}(t) \in \Re^2$ as the difference between the subsequently designed auxiliary signal $z_d(t) \in \Re^2$ and the transformed variable $z(t)$ defined in Eq. (18) as follows:

$$\tilde{z} = z_d - z \tag{23}$$

Based on the structure of the open-loop error system given by Eqs. (17) and (18) and the subsequent stability analysis, we design the kinematic control input $\boldsymbol{u}(t)$ as

$$\boldsymbol{u} = -k_pe_0z + [\omega_{d2} \quad \omega_{d3}]^T + \boldsymbol{u}_a \tag{24}$$

where $k_p(t) \in \Re^1$ is a gain constant, $\boldsymbol{u}_a(t) \in \Re^2$ is an auxiliary control signal that is defined as

$$\boldsymbol{u}_a = \Pi_0J_2z_d + \Pi_1z_d \tag{25}$$

and where the auxiliary signal $z_d(t) \in \Re^2$ is defined by the following oscillatorlike relationship,

$$\dot{z}_d = (\dot{\delta}_d/\delta_d)z_d + \Lambda J_2z_d, \qquad z_d^T(0)z_d(0) = \delta_d^2(0) \tag{26}$$

and where the auxiliary terms $\Pi_0(t)$, $\Pi_1(t)$, $\Lambda(t)$, and $\delta_d(t) \in \Re^1$ are defined as

$$\Pi_0 = (k_ax + e_0\tilde{\omega}_1)/\delta_d^2 \tag{27}$$

$$\Pi_1 = 2\dot{\delta}_d/e_0\delta_d + k_pe_0 \tag{28}$$

$$\Lambda = \tfrac{1}{2}(k_pe_0x + e_0\Pi_0 + \tilde{\omega}_1) \tag{29}$$

$$\delta_d = \gamma_0\exp(-\gamma_1t) + \varepsilon_1 \tag{30}$$

where $k_a$, $\gamma_0$, $\gamma_1$, and $\varepsilon_1 \in \Re^1$ are positive, constant design parameters.

*Remark 4:* Motivation for the structure of Eq. (26) is obtained by taking the time derivative of $z_d^Tz_d$ as

$$\frac{\mathrm{d}}{\mathrm{d}t}\left(z_d^Tz_d\right) = 2z_d^T\dot{z}_d = 2z_d^T\left(\frac{\dot{\delta}_d}{\delta_d}z_d + \Lambda J_2z_d\right) = 2\frac{\dot{\delta}_d}{\delta_d}z_d^Tz_d \tag{31}$$

where Eq. (26) and the definition of Eq. (22) have been utilized. As a result of the selection of the initial conditions given in Eq. (26), it is easy to verify that

$$z_d^Tz_d = \|z_d\|^2 = \delta_d^2 \tag{32}$$

solves the differential equation given in Eq. (31).

To obtain the closed-loop error system for $x(t)$, we substitute Eq. (24) for $\boldsymbol{u}(t)$ in Eq. (17) and then perform some algebraic manipulations to obtain

$$\dot{x} = -\tfrac{1}{2}k_a x - \tfrac{1}{2}\tilde{z}^T J_2 \boldsymbol{u}_a \tag{33}$$

To determine the closed-loop error system for $\tilde{z}(t)$, we take the time derivative of Eq. (23), substitute Eqs. (26) and (18) for $\dot{z}_d(t)$ and $\dot{z}(t)$, respectively, and finally substitute Eq. (24) for $u(t)$ to obtain

$$\dot{\tilde{z}} = \tfrac{1}{2}\left[-k_p e_0^2 \tilde{z} + J_2\tilde{z}(\tilde{\omega}_1 + k_p e_0 x) + x J_2 \boldsymbol{u}_a\right] \tag{34}$$

where common terms have been canceled and the skew-symmetry of the matrix $J_2$ has been used.

## Stability Analysis

*Theorem:* Given the closed-loop system of Eqs. (33) and (34), the kinematic controller of Eqs. (24–30) ensures UUB tracking in the sense that

$$\|\boldsymbol{e}(t)\| \le \lambda_1 \exp(-\lambda_2 t) + \lambda_3 \varepsilon_1 \tag{35}$$

for all initial conditions such that

$$0 \le \|e(0)\| \le [\delta - 8(\gamma_0 + \varepsilon_1)]/9 \tag{36}$$

where $\lambda_1$, $\lambda_2$, $\lambda_3$, and $\delta \in \Re^1$ are some positive constants and $\gamma_0$ and $\varepsilon_1$ were originally introduced in Eq. (30). Note that $\gamma_0$ and $\varepsilon_1$ must be selected sufficiently small to ensure that Eq. (36) can be satisfied.

*Proof:* To prove the theorem, we define a nonnegative, scalar function, denoted by $V(t) \in \Re^1$, as

$$V = x^2 + \tilde{z}^T\tilde{z} \tag{37}$$

After taking the time derivative of Eq. (37) and making the appropriate substitutions from Eqs. (33) and (34), we obtain the following expression:

$$\dot{V} = x\left[-k_a x - \tilde{z}^T J_2 \boldsymbol{u}_a\right] + \tilde{z}^T\left[-k_p e_0^2\tilde{z} + J_2\tilde{z}(\tilde{\omega}_1 + k_p e_0 x) + x J_2 \boldsymbol{u}_a\right] \tag{38}$$

After canceling common terms in Eq. (38), we can obtain a simplified expression for $\dot{V}(t)$ in the following manner:

$$\dot{V} = -k_a x^2 - k_p e_0^2 \tilde{z}^T\tilde{z} \tag{39}$$

We can now utilize Eqs. (37) and (39) to find a negative–definite upper bound for $\dot{V}(t)$ as

$$\dot{V} \le -\beta V \qquad \text{if} \qquad |e_0(t)| \ge \delta_1 > 0 \tag{40}$$

where $\beta \in \Re^1$ is some positive constant and $\delta_1$ is a strictly positive constant that can be picked arbitrarily small. After applying Eq. (16) to the inequality constraint in Eq. (40) and solving the preceding differential inequality, we obtain the following sufficient condition for the solution of $V(t)$:

$$V(t) \le \exp(-\beta t)V(0) \qquad \text{if} \qquad \|\boldsymbol{e}(t)\| \le \delta \tag{41}$$

where $\delta = \sqrt{(1-\delta_1^2)}$ is another positive constant. After utilizing Eqs. (19) and (37), we can rewrite Eq. (41) as follows

$$\|\boldsymbol{\zeta}(t)\| \le \exp[-(\beta/2)t]\|\boldsymbol{\zeta}(0)\| \qquad \text{if} \qquad \|x(t)\| + 2\|z(t)\| \le \delta \tag{42}$$

where $\boldsymbol{\zeta}(t) \in \Re^3$ is defined as

$$\boldsymbol{\zeta} = [x \quad \tilde{z}^T]^T \tag{43}$$

To continue the proof, we note that $\|z(t)\|$ can be upper bounded by applying the triangle inequality to Eq. (23) as follows:

$$\|z\| \le \|\tilde{z}\| + \|z_d\| \le \|\tilde{z}\| + \gamma_0 + \varepsilon_1 \tag{44}$$

where Eq. (30) has been utilized. We can now utilize the bound developed in Eq. (44) to obtain a sufficient condition for Eq. (42) as follows:

$$\|\boldsymbol{\zeta}(t)\| \le \exp[-(\beta/2)t]\|\boldsymbol{\zeta}(0)\| \qquad \text{if} \qquad \|x(t)\| + 2\|\tilde{z}\| + 2(\gamma_0 + \varepsilon_1) \le \delta \tag{45}$$

We now utilize the definition of Eq. (43) to obtain a sufficient condition for Eq. (45) as follows:

$$\|\boldsymbol{\zeta}(t)\| \le \exp[-(\beta/2)t]\|\boldsymbol{\zeta}(0)\| \qquad \text{if} \qquad \|\boldsymbol{\zeta}(t)\| \le [\delta - 2(\gamma_0 + \varepsilon_1)]/3 \tag{46}$$

We can now utilize Eq. (46) to note that the following inequality would always be valid:

$$\|\boldsymbol{\zeta}(t)\| \le \|\boldsymbol{\zeta}(0)\| \qquad \text{if} \qquad \|\boldsymbol{\zeta}(t)\| \le [\delta - 2(\gamma_0 + \varepsilon_1)]/3 \tag{47}$$

The inequalities described by Eq. (47) essentially imply that $\|\boldsymbol{\zeta}(t)\|$ is upperbounded by $\|\boldsymbol{\zeta}(0)\|$ if $\|\boldsymbol{\zeta}(t)\|$ is also upperbounded by $[\delta - 2(\gamma_0 + \varepsilon_1)]/3$. Because $\|\boldsymbol{\zeta}(0)\|$ is a constant that can be independently restricted (a measure of the initial error between the desired and system orientations), we can upperbound $\|\boldsymbol{\zeta}(0)\|$ by $[\delta - 2(\gamma_0 + \varepsilon_1)]/3$ to satisfy both upperbounds on $\|\boldsymbol{\zeta}(t)\|$ described earlier by Eq. (47). Mathematically, this implies

$$\|\boldsymbol{\zeta}(t)\| \le \|\boldsymbol{\zeta}(0)\| \qquad \text{if} \qquad \|\boldsymbol{\zeta}(0)\| \le [\delta - 2(\gamma_0 + \varepsilon_1)]/3 \tag{48}$$

Now, we can utilize Eqs. (46), (48), and (43) to obtain

$$\|x\|, \|\tilde{z}\| \le \exp[-(\beta/2)t]\|\boldsymbol{\zeta}(0)\| \qquad \text{if} \qquad \|\boldsymbol{\zeta}(0)\| \le [\delta - 2(\gamma_0 + \varepsilon_1)]/3 \tag{49}$$

We now use the triangle inequality and Eqs. (30) and (49) to obtain the following bound for $z(t)$:

$$\|z\| \le \|\tilde{z}\| + \|z_d\| \le \exp[-(\beta/2)t]\|\boldsymbol{\zeta}(0)\| + \gamma_0\exp(-\gamma_1 t) + \varepsilon_1 \qquad \text{if} \qquad \|\boldsymbol{\zeta}(0)\| \le [\delta - 2(\gamma_0 + \varepsilon_1)]/3 \tag{50}$$

The inequality given by Eq. (35) can now be directly obtained from the leftmost inequalities given in Eqs. (49) and (50). From Eq. (49), it is straightforward to see that $x(t), \tilde{z}(t) \in \mathcal{L}_\infty$. From Eqs. (32) and (50), we can conclude that $\boldsymbol{z}(t)$, $z_d(t) \in \mathcal{L}_\infty$. Based on that $x(t)$, $z(t) \in \mathcal{L}_\infty$ and that the reference trajectory is selected so that $q_{0d}(t)$, $\boldsymbol{q}_d(t) \in \mathcal{L}_\infty$, we can utilize Eqs. (19), (10), and (11) to conclude that $\boldsymbol{q}(t), q_0(t) \in \mathcal{L}_\infty$. By virtue of Remark 3 and Eq. (13), it is easy to see that $\boldsymbol{\omega}_d(t) \in \mathcal{L}_\infty$. From the earlier assertion and the fact that $\omega_1(t)$ is assumed to stay bounded, we can utilize Eq. (12) to show that $\tilde{\omega}_1(t) \in \mathcal{L}_\infty$. Using the preceding boundedness assertions, we can conclude that $f(t) \in \mathcal{L}_\infty$ from Eq. (20). Based on these facts, we can now utilize Eqs. (24–30) to show that $\boldsymbol{u}(t)$, $\boldsymbol{u}_a(t)$, $\dot{z}_d(t)$, $\Pi_0(t)$, $\Pi_1(t) \in \mathcal{L}_\infty$. Because $\boldsymbol{u}(t) = [\omega_2(t) \quad \omega_3(t)] \in \Re^2$ is the kinematic control input vector, it is possible to state that the control input remains bounded for all time.

Independent of the proof of the inequality of Eq. (35), we will now proceed to show how the initial condition restrictions on $\boldsymbol{\zeta}(t)$ correspond to initial condition restrictions on the actual tracking error variables, that is we want to prove the inequality given by Eq. (36). We utilize the definition of Eq. (43) to relate $\|\boldsymbol{\zeta}(0)\|$ to $\|\boldsymbol{e}(0)\|$ in the following manner:

$$\|\boldsymbol{\zeta}(0)\| \le 3\|\boldsymbol{e}(0)\| + 2(\gamma_0 + \varepsilon_1) \tag{51}$$

where the definitions of Eqs. (23) and (30) have been utilized. After substituting Eq. (51) for $\|\boldsymbol{\zeta}(0)\|$ in the rightmost inequality given in Eq. (50), we can arrive at the sufficient condition given in Eq. (36) where we have utilized that $\exp(-\beta t)$ and $\exp(-\gamma_1 t)$ can be upper bounded by one. □

*Remark 5:* As a direct consequence of the expression of Eq. (40) and the initial condition magnitude restriction given in Eq. (36), we are guaranteed that $e_0(t) \neq 0 \,\forall t$; hence, the control singularity at $e_0(t) = 0$ [see the definition of $\Pi_1(t)$ of Eq. (28)] will always be avoided.

*Remark 6:* The initial condition magnitude restriction given in Eq. (36) can be viewed as a restriction on the desired unit quaternion, denoted by $\boldsymbol{q}_{dE}(t)$, as can be seen from the definition of $\boldsymbol{e}(t)$ given in Eq. (11), that is, given the initial state of the system $\boldsymbol{q}_E(0)$, one must select $\boldsymbol{q}_{dE}(0)$ such that $\|\boldsymbol{e}(0)\|$ satisfies the sufficient condition given in Eq. (36).

*Remark 7:* Because the kinematic controller is designed to be differentiable, standard backstepping techniques[10] can be utilized to design the torque control input vector for the dynamic model of an underactuated axisymmetric spacecraft.[7]

*Remark 8:* As a special case of the tracking problem, we consider the case of exact regulation of the orientations of the three axes to the origin. When $\omega_1(t)$ has a nonzero value, it is easy to see from Eq. (14) that exact three-axis stabilization is not possible. However, the proposed control law ensures that the orientation of the spacecraft can be driven to an arbitrarily small neighborhood of the origin.

## Simulation Results

In this section, we present a numerical simulation to validate the controller of Eqs. (24–26) applied to the full-order model of an underactuated axisymmetric spacecraft given by Eqs. (1), (2),

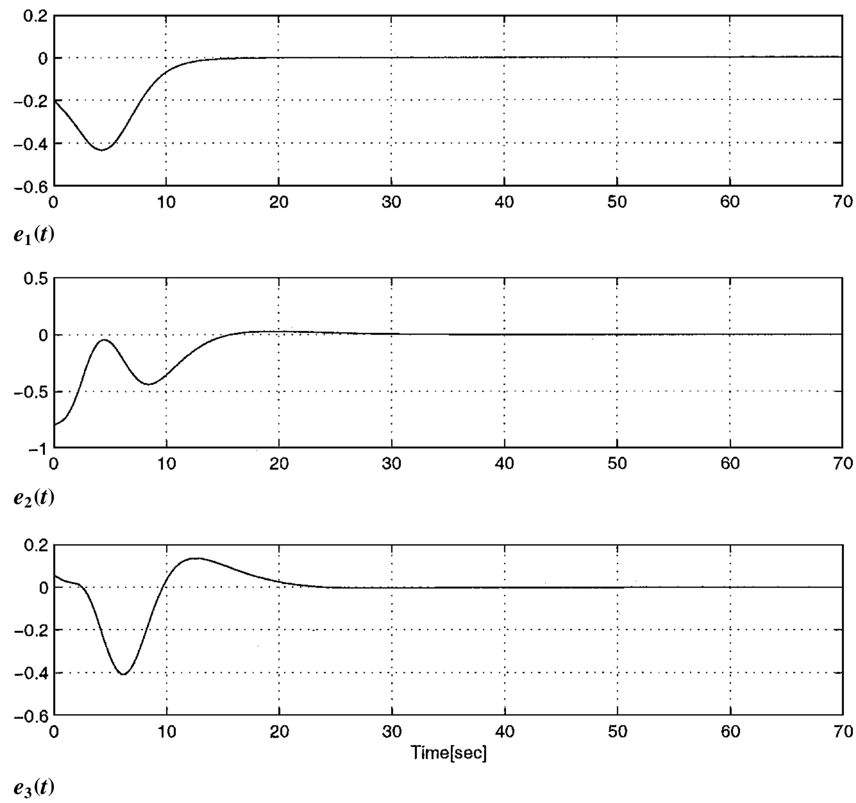


**Fig. 1 Orientation error.**

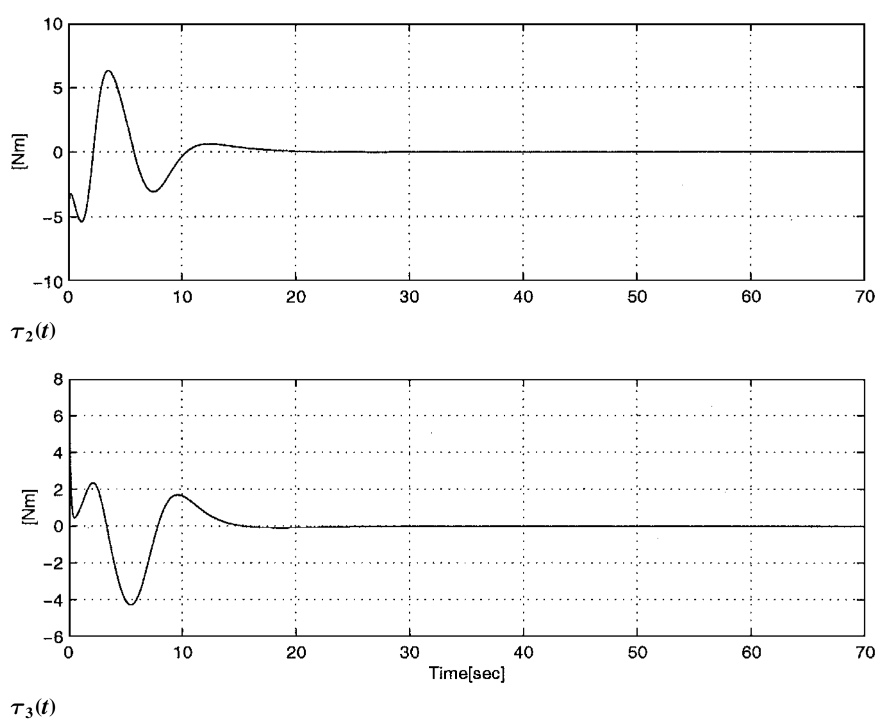


**Fig. 2 Applied torque.**

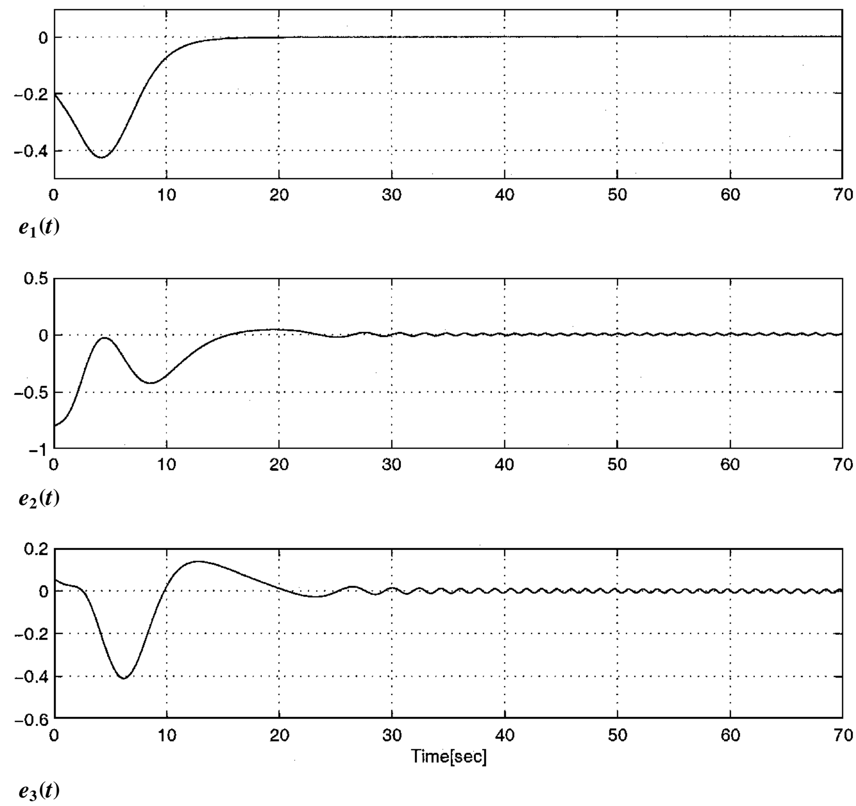


**Fig. 3 Orientation error.**

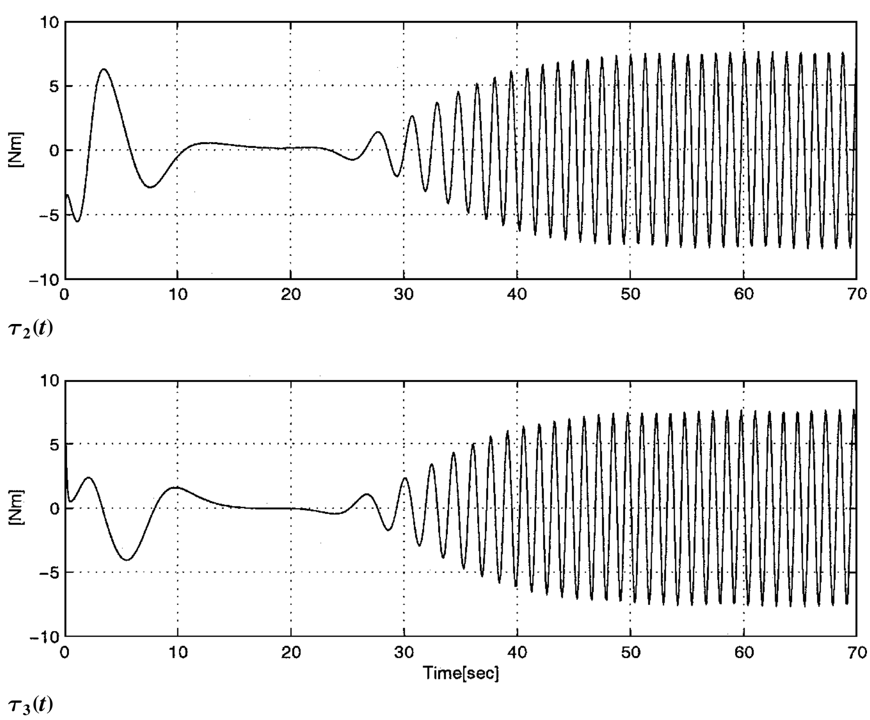


**Fig. 4 Applied torque.**

and

$$j_1\dot{\omega}_1 = 0 \tag{52}$$

$$j_2\dot{\omega}_2 = (j_3 - j_1)\omega_1\omega_3 + \tau_2 \tag{53}$$

$$j_3\dot{\omega}_3 = (j_1 - j_2)\omega_1\omega_2 + \tau_3 \tag{54}$$

where $j_1 = 20$ kgm$^2$ and $j_2 = j_3 = 15$ kgm$^2$ represent the inertia parameters for the axisymmetric spacecraft.

The aim of the first simulation study was to regulate the spacecraft orientation to a UUB neighborhood of the desired orientation specified as

$$q_{0d} = \sqrt{0.1}, \qquad \boldsymbol{q}_d = \begin{bmatrix}\sqrt{0.4} & \sqrt{0.25} & \sqrt{0.25}\end{bmatrix}^T$$

The initial attitude of the spacecraft was set to

$$q_0(0) = \sqrt{0.1}, \qquad \boldsymbol{q}(0) = \begin{bmatrix}0 & -\sqrt{0.45} & -\sqrt{0.45}\end{bmatrix}^T \tag{55}$$

such that the unit quaternion constraint is satisfied. The initial value for $\omega_1(t)$ was chosen to be zero. The auxiliary signal $z_d(t)$ was

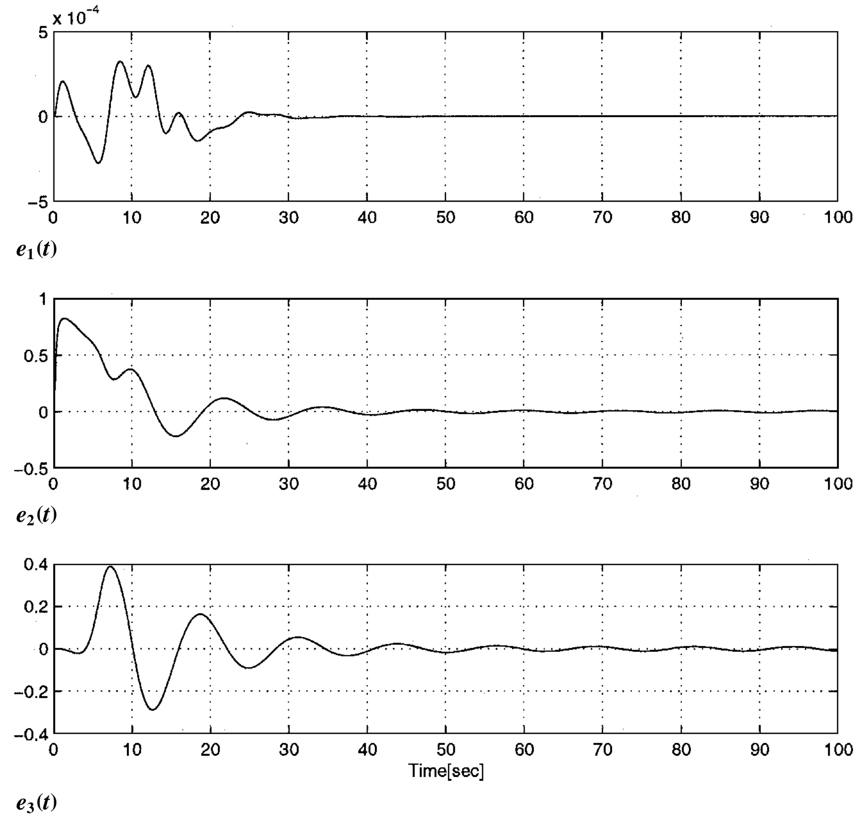


**Fig. 5 Orientation tracking error.**

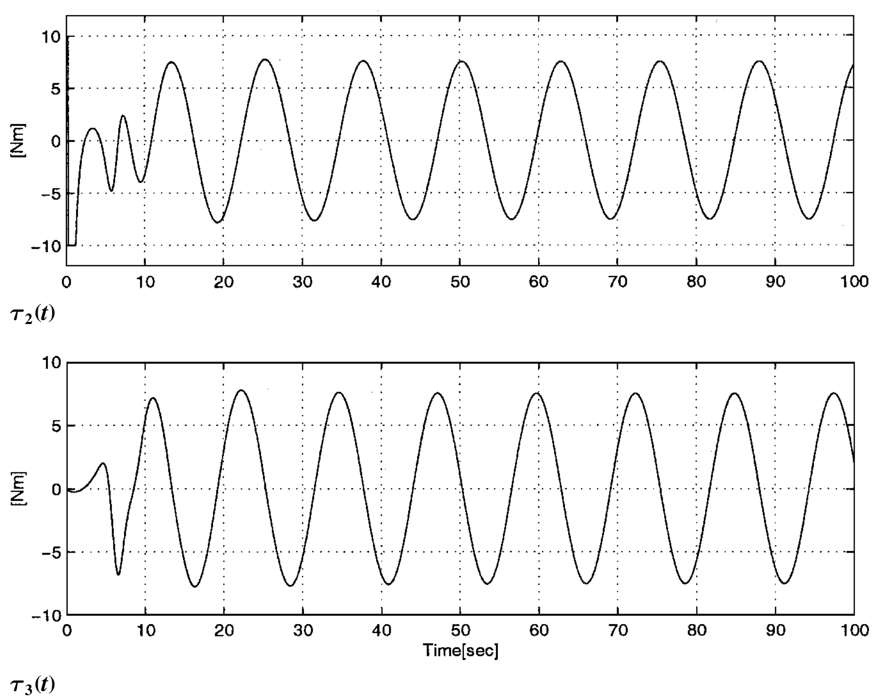


**Fig. 6 Applied torque.**

initialized to be $[2.001 \quad 0]^T$. The control gains that resulted in the best regulation are

$$k_p = 0.8, \qquad k_a = 0.8, \qquad \gamma_0 = 2.0, \qquad \gamma_1 = 0.2$$

$$\varepsilon_1 = 0.001, \qquad k_1 = 10.0, \qquad k_2 = 10.0 \tag{56}$$

From Fig. 1, we can see that the orientation of the spacecraft is UUB regulated to the origin. From Fig. 2, the torques remain bounded for all times. In the next run of the simulation, $\omega_1(t)$ was chosen to have a small initial value of 0.001 $\text{rad}^{-1}$. The system was simulated with the same set of inertia parameters, initial conditions, desired orientation, and control gains save $\varepsilon_1$, which was chosen to be 0.01 to keep the torques within reasonable amplitudes. From Fig. 3, we can see that the regulation control objective has been achieved. As already mentioned in Remark 8, the orientation cannot be regulated exactly to the origin. However, UUB regulation is achieved as expected. From Fig. 4, the torques remain bounded. As the orientation trajectories converge to a neighborhood of the origin, the torques do get larger in amplitude; however, this is the cost that is paid for allowing the unactuated $\omega_1(t)$ to have a finite value.

This second simulation study forces the spacecraft orientation to track a desired trajectory that is generated via the desired dynamics of Eqs. (6) and (7) utilizing $\bar{\omega}_d(t)$ as input. We select $\bar{\omega}_d(t)$ to be a soft start trajectory in the following manner:

$$\bar{\omega}_d(t) = \{0 \quad [1-\exp(-0.01t^2)]\sin(0.5t) \quad [1-\exp(-0.01t^2)]\cos(0.5t)\}^T \tag{57}$$

The initial conditions for the desired and actual attitude of the spacecraft were selected as

$$q_0(0) = q_{0d}(0) = \sqrt{0.1}$$
$$\boldsymbol{q}(0) = \boldsymbol{q}_d(0) = \begin{bmatrix}0 & \sqrt{0.45} & \sqrt{0.45}\end{bmatrix}^T \tag{58}$$

such that the unit quaternion constraint is satisfied. The initial value for $\omega_1(t)$ was chosen to be 0 rad$^{-1}$. We notice here that $\bar{\omega}_{d1}(t) = \omega_1(0) = 0$. The auxiliary signal $z_d(t)$ was initialized to be $[1.01 \quad 0]^T$. The control gains that resulted in the best tracking performance are

$$k_p = 10.0 \qquad k_a = 0.5 \qquad \gamma_0 = 1.0 \qquad \gamma_1 = 0.1$$
$$\varepsilon_1 = 0.01 \qquad k_1 = 20.0 \qquad k_2 = 20.0 \tag{59}$$

The torques were saturated to remain $\pm 10$ N · m. From Fig. 5, we can see that the spacecraft orientation tracks the desired trajectory to a UUB neighborhood. From Fig. 6, the torques remain bounded for all times. Note that the UUB neighborhood can always be reduced by selecting $\varepsilon_1$ to be a smaller value.

## Conclusions

In this Note, we have presented a nonlinear controller for the attitude tracking problem for a rigid underactuated spacecraft. For the reduced-order problem, that is, the spacecraft dynamics are neglected, the controller achieved uniformly ultimately bounded tracking provided the initial tracking errors are selected sufficiently small. Simulation results for the controller demonstrated the efficacy of the proposed strategy in achieving tracking for the underactuated spacecraft.

## Acknowledgments

This work is supported in part by National Science Foundation Grant DMI-9457967, Office of Naval Research Grant N000014-99-1-0589, a Department of Commerce Grant, and an Army Research Office Automotive Center Grant. The authors would like to thank the reviewers for their constructive suggestions and a careful review of the manuscript.

## References

[1]Crouch, P., "Spacecraft Attitude Control and Stabilization: Applications of Geometric Control Theory to Rigid Body Models," *IEEE Transactions on Automatic Control*, Vol. 29, No. 4, 1984, pp. 321–331.

[2]Byrnes, C., and Isidori, A., "On the Attitude Stabilization of Rigid Spacecraft," *Automatica*, Vol. 27, No. 1, 1991, pp. 87–95.

[3]Brockett, R., "Asymptotic Stability and Feedback Stabilization," *Differential Geometric Control Theory*, edited by R. Brockett, R. Millman, and H. Sussmann, Birkhäuser Boston, Cambridge, MA, 1983, pp. 181–191.

[4]Morin, P., Samson, C., Pomet, J., and Jiang, Z., "Time-Varying Feedback Stabilization of the Attitude of a Rigid Spacecraft with Two Controls," *Systems and Controls Letters*, Vol. 25, No. 5, 1995, pp. 375–385.

[5]Coron, J., and Kerai, E., "Explicit Feedbacks Stabilizing the Attitude of a Rigid Spacecraft with Two Control Torques," *Automatica*, Vol. 32, No. 5, 1996, pp. 669–677.

[6]Morin, P., and Samson, C., "Time-Varying Exponential Stabilization of a Rigid Spacecraft with Two Control Torques," *IEEE Transactions on Automatic Control*, Vol. 42, No. 4, 1997, pp. 528–534.

[7]Tsiotras, P., and Luo, J., "Control of Underactuated Spacecraft with Bounded Inputs," *Automatica*, Vol. 36, No. 8, 2000, pp. 1153–1169.

[8]Dixon, W. E., Dawson, D. M., Zergeroglu, E., and Zhang, F., "Robust Tracking and Regulation Control for Mobile Robots," *International Journal of Robust and Nonlinear Control: Special Issue on Control of Underactuated Nonlinear Systems*, Vol. 10, No. 4, 2000, pp. 199–216.

[9]Hughes, P., *Spacecraft Attitude Dynamics*, Wiley, New York, 1986, pp. 17–31.

[10]Krstić, M., Kanellakopoulos, I., and Kokotovic, P., *Nonlinear and Adaptive Control Design*, Wiley, New York, 1995, pp. 19–86.

# Method of Unsteady Aerodynamic Forces Approximation for Aeroservoelastic Interactions

Iulian Cotoi* and Ruxandra M. Botez†
*Ecole de Technologie Supérieure, Montréal, Quebec H3C 1K3, Canada*

## Introduction

THE adverse interactions occurring between the three main disciplines unsteady aerodynamics, aeroelasticity, and servocontrols are called aeroservoelastic interactions. These interactions can be described mathematically by a system of equations in a state-space form. This system requires a different representation for the unsteady aerodynamic forces from that for the classical flutter equation. The unsteady aerodynamic forces, in the case of the classical flutter equation or aeroelasticity, are calculated by the doublet lattice method (DLM) in the frequency domain for a set of reduced frequencies $k$ and Mach numbers $M$. Because time-domain linear time-invariant ordinary differential equations (LTI ODE) are required for using modern control theory design, several approximations for the unsteady aerodynamic forces in the $s$ domain have been developed. There are mainly three formulations to approximate the unsteady generalized forces by rational functions in the Laplace domain in the frequency domain[1–4]: least square (LS), modified matrix Padé, and minimum state (MS). The approximation yielding the smallest order time-domain LTI state-space model is the MS (Ref. 5) approximation method. The dimension of the time-domain LTI state-space model depends on the number of retained modes and the number of aerodynamic lags $n_a$. There is a tradeoff between the number of aerodynamic lags and the accuracy of the approximation. The higher the $n_a$, the better the approximation, but the order of the time-domain LTI state-space model is larger. The order of the LTI state-space model strongly affects the efficiency of subsequent analyses. In the present Note a new method for the determination of efficient state-space aeroservoelastic models is presented. This method combines results from the theory of Padé approximants and the theory of model reduction developed in the frame of control theory. Finally, a comparison between the new method and the MS method is presented. The error of our method is 12–40 times smaller than the error of the MS approximation method for the same number of augmented states $n_a$ and depends on the choice of the model reduction method.

## Aircraft Equations of Motion

The motion of an aircraft modeled as a flexible structure with no forcing terms is described by the following equations, written in the time-domain:

$$\tilde{\boldsymbol{M}}\ddot{\eta} + \tilde{\boldsymbol{C}}\dot{\eta} + \tilde{\boldsymbol{K}}\eta + q_{\text{dyn}}\boldsymbol{Q}(k)\eta = 0 \tag{1}$$

Here $\eta$ is the generalized variable defined as $\boldsymbol{q} = \boldsymbol{\Phi}\eta$, where $\boldsymbol{q}$ is the displacement vector and $\boldsymbol{\Phi}$ is the matrix formed with the

Received 20 July 2001; revision received 1 March 2002; accepted for publication 7 March 2002. 

*Postdoctoral Fellow.
†Professor, Automated Production Department. Member AIAA.